Experimental Analysis of the Flow over a Wing under Ground and Down Force Effects

Pedro Henrique Bernardi Franzini[1] and Odenir de Almeida[1]

[1]*Universidade Federal de Uberlândia – Faculdade de Engenharia Mecânica – Centro de Pesquisa em Aerodinâmica Experimental (CPAERO) – Uberlândia/MG – Brazil.*

Corresponding Author: Odenir de Almeida | Universidade Federal de Uberlândia – Faculdade de Engenharia Mecânica – Centro de Pesquisa em Aerodinâmica Experimental | BR 050 km 78 – Campus Gloria | CEP: 38.410-337 – Uberlândia/MG – Brazil.

ABSTRACT

The principal aim of this study is to investigate the correlation between the negative lift force, commonly referred to as down force, generated by cambered low aspect ratio (AR = 2.63) wing designed for racing car applications, and its proximity to the ground, thereby characterizing the ground effect. Furthermore, aerodynamic drag force and the aerodynamic performance of the wing in the presence and absence of wingtip plates, known as endplates, were evaluated under these conditions. To achieve these objectives, an equipped low-speed subsonic wind tunnel setup with an aerodynamic balance, a Pitot-tube and anemometer, and a physical assembly of the wing integrated with the measurement system was employed. Results were very consistent and demonstrate that for small distances to the ground, enough down force was produced within a range of ground clearance (h/c) between 0.2 and 0.4 while viscous effects were also present for jeopardizing the benefits at some specific conditions. The use of endplates has increased the Lift by a factor of 8.3%.

Keywords: *Down force, Ground Effect, Endplate, Cambered Airfoil, Car Aerodynamics.*

INTRODUCTION

After decades of advancements in our understanding of wings and airfoils in the aeronautical industry, the 20th century, particularly the 1960s, marked a significant turning point when engineers and race car designers began to take a keen interest in wing concepts. They observed the lift effects seen in airplanes and recognizing similarities between the high speeds of their racing cars and the demand for rapid maneuverability in competitions, conceiving the idea of inverting the wing to generate negative lift. This inverted wing was then affixed to the car with the primary objective of augmenting the normal force between the car's wheels and the ground. This substantial increase in grip between the rubber tires and the road surface translated to a significant enhancement in the car's speed and handling during turns. This phenomenon of generating negative lift came to be known as 'downforce'.

The Formula One (F-1) car that first featured an attached wing was the Lotus 49 – Fig. 1. This evolution in race car design is well-documented by Katz in his work on race car wings [1].

Figure 1. *The Lotus 49 F1-race car with rear wing.*

Source: https://c-magazine.com/features/extra-time/aerodynamics-1968-1970.

From then on, downforce-focused airfoils continued to be developed and used both in single-seater categories, such as F-1 itself or IndyCar, and in sports street cars, such as Bugatti

– Fig.2, Ferrari, Porsche, Mercedes, Lamborghini, and others. However, another important aspect brought from the aeronautical industry is the proximity of the wing and the ground. The concept of ground effect became more widely recognized and studied as aircraft technology advanced and aviation research expanded. In the same way, it wasn't until the mid-20th century that more comprehensive research and testing were conducted to quantify the effects of ground effect on aircraft performance.

Figure 2. *Bugatti Veyron with rear wing.*

Source:https://newsroom.bugatti.com/press-releases/all-the-way-to-china-at-408-84-km-h-bugatti-celebrates-the-international-debut-of-the-world-s-fastest-open-top-production-sports-car-at-the-shanghai-motor-show
https://newsroom.bugatti.com/press-releases/all-the-way-to-china-at-408-84-km-h-bugatti-celebrates-the-international-debut-of-the-world-s-fastest-open-top-production-sports-car-at-the-shanghai-motor-show

As for automotive aerodynamics, basically all concepts arising from the aeronautical industry in this subject can be extrapolated and adapted for motorsport: a rear wing with an optimized C_L/C_D ratio to produce down force will keep the vehicle with more grip on the ground, improving its rear stability and its performance in curves when compared to the vehicle without the presence of the wing.

There are, therefore, major challenges in terms of aerodynamics for the design of a prototype of a wing to evaluate the ground effect as present in racing cars, such as: a) The relationship between the length of the airfoil chord (c) and its height above the ground or clearance (h); b) The effects of inserting and removing endplates; c) The way the wing is attached to the car, which needs to interfere with the airflow as little as possible in order to not produce an unwanted drag force; d) The airfoil manufacturing process, as it has a complex geometry; e) The effects of roughness on the surface of the airfoil, which, according to the theory of fluid mechanics, must have the lowest possible roughness in order to have high efficiency of the aerodynamic properties of the airfoil.

A great contribution in this field is attributed to [1]. The down force reduction effect evaluated in the literature is a characteristic of the $C_L \times h/c$ curve in which the proximity to the ground initially increases the lift coefficient. But for regions very close to the ground, reaches a maximum and reduces the C_L again, which is limited by viscous effects taking place. The work of [2] points out that the phenomenon of down force reduction to very low h/c is due to the combination of the gradual separation effects of the boundary layer limit due to the high gradient in pressure recovery generated by the effect venturi and the slight reduction in pressure in the pressure surface.

Another important feature to note is the increase in the growth rate of C_L with proximity to the ground through the evolution of this pressure effect on the outer regions of the wing. This effect is attributed to the suction induced by the vortex generated at the edge of the endplate, known as the edge vortex. Due to the pressure difference between the sides of the endplate, there is infiltration of airflow from the outer endplate region to the lower low pressure inner region of the wing [3].

Despite the important findings, these works were placed in the past almost one decade ago. The most recent research on this subject is given by [4] which evaluated the aerodynamics characteristics of an inverted single element CLARK-Y airfoil with and without ground effect showing that the C_L increased with angle of attack except the angles of attack larger than 10° and with ground effects except at ride heights of less than 0.1c due to the force reduction phenomena.

Other examples of experimental works are seen in [5-6], where in the first study the aerodynamics

and tip vortex flow of a rectangular wing at moderate Re number was carried out, while in the second the aerodynamics of sinusoidal leading-edge wings was investigated underground effect for a wide range of angle of attack at very low Reynolds number. Both academic research verified a large lift increase with reducing ground distance.

Computational approaches for investigating wings and airfoils at ground effect are also seen in literature. As example, the work of [7] investigated numerically the effect of rubber debris on an inverted double element wing in ground effect at representative Reynolds numbers. It was found that debris near the center of the wing-element has a greater impact. Also, the changes of the lift-to-drag ratio of an airfoil NACA4412 with the variation of ground clearance and angles of attack was simulated by [8]. Without 3D effects, not simulated, results confirmed that the lower the ground clearance, the higher the lift-to-drag ratio. Also, numerical investigation on the aerodynamic efficiency of bio-inspired corrugated and cambered airfoils in ground effect was presented by [9]. This research numerically investigated the flapping motion effect on the flow around two subsonic airfoils near a ground wall indicating a direct relationship between the airfoil's aerodynamic performance (cl/cd) and the ground effect.

Lee and Lin [10] revealed a most recent review of experimental works of wings in ground effect and at low Re numbers. In this work the authors presented data for rectangular and delta wings of reverse and regular configurations. For rectangular wings, both chord-dominated and span-dominated ground effects on the aerodynamics, tip vortex, and lift-induced drag are reviewed. Suggestions for future investigations applicable to each wing planform in ground effect are provided.

Despite the valuable studies that were performed so far, there are still some gaps that should be filled. The aim of this research is to investigate a low-aspect ratio cambered wing in ground effect with the addition of endplate effects. To accurately characterize the problem, the tests were carried out under controlled conditions with a wind tunnel, movable wing, and use of aerodynamics balance for registering lift and drag forces. Systematic data were collected to examine the effect of variation of clearance to the ground and angle of attack under the effect of the endplates. A second test was carried out to evaluate the variation of clearance and presence of endplates with a fixed AOA.

In the subsequent sections of this paper, we will delve into our methodology, experimental setup, results, and discussion of the most important findings. By shedding light on the ground effect in a low aspect ratio wing, the main contribution of this study is to provide more extensive information about such wings and its performance. Ultimately, the focus was kept to the understanding of the wing and ground flow interaction at low ground clearance.

EXPERIMENTAL SETUP

Test Article

The investigated wing is constructed with an E423 airfoil, as depicted by Fig.3. Such an airfoil should be efficient at a low Reynolds number and have its curvature compliant with the production of down force. The Eppler family airfoils are historically used in wing analysis in vehicle aerodynamics, as they have a more asymmetrical and more cambered line, which favors the pressure differential at lower speeds and angles of attack in relation to typical aircraft airfoils.
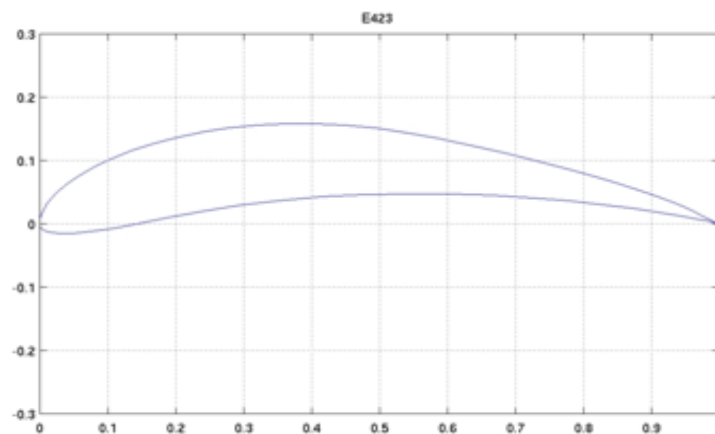
Figure 3. *Investigated airfoil profile used in the low-aspect ratio wing.*

The dimensions of the wing were defined as the chord measuring 190 mm with its span measuring 500 mm giving an aspect ratio (AR) of 2.63. The whole wing was composed of three parts that were 3D-printed in PLA by using a Replicator Z18 machine. The pieces have been united in one

and surface finishing was achieved by using automotive painting-pattern for smoothing the surface and to provide high quality. There is a recess in the center of the wing to support the model downstream of the wind tunnel flow in the vertical and adjustable position. The rod attached the wing in the aerodynamic balance, completely vertical and rigid, precisely to transfer the load coming from the airfoil to the balance, accurately confirming the measurement of its forces – Fig.4.

Figure 4. *General assembly of the wing with rod support.*

During the experiments the minimum height or ground clearance value was kept at $H_{rod} = 38$ mm which corresponds to h/c = 0.2, due to the assembly limitation. The expected thickness of the boundary layer by the flow developed on the ground (δ_{TB}) was estimated with the following equation from [11]:

$$\delta_{TB} = 5 \frac{x}{\sqrt{Re_x}} \qquad (1)$$

Where x is the maximum longitudinal distance until the flow reach the wing location, so it can be approximated to the total size of $x = 1.510$ m. Thus, assuming the wind tunnel speed of 22 m/s and considering a high temperature of 30ºC, making the coefficient of kinematic viscosity

$\nu = 15.98 \times 10^{-6}$ m²/s; the value of $\delta_{TB} \approx 5$ mm.

Endplates

According to the patent from [12], endplates do not need to be too elaborate or complex for their effects to be relevant to the aerodynamic efficiency of the wing. In this way, a very simple endplate model was built. The shape of the endplate would initially be rectangular, but to avoid proximity or contact with the ground at very high angle of attack in low ground clearance (h/c), the forward-facing lower edge of it was rounded. The endplates were made by a 2 mm acrylic sheet and cut in the shape as depicted by Fig. 5.
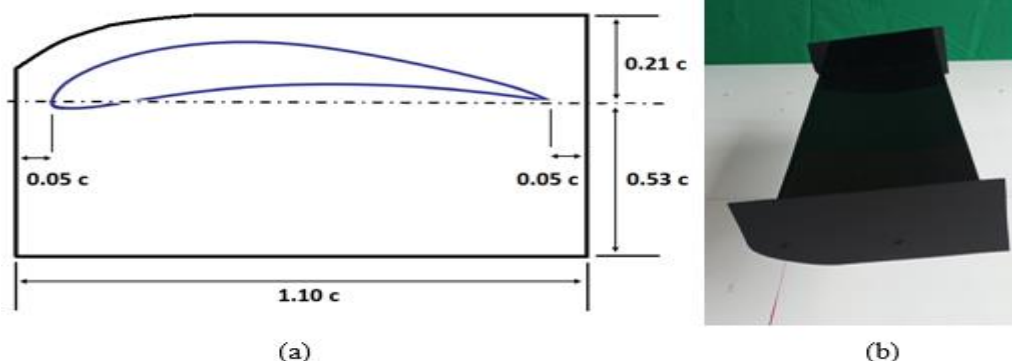
Figure 5. *Endplate dimensions sketched (a) and the final model (b).*

The Wind Tunnel Setup

The tests were carried out in an open section subsonic wind tunnel called TV60 in the Experimental Aerodynamics Laboratory (LAEX), as part of Experimental Aerodynamics Research Center (CPAERO) from Federal University of Uberlandia (UFU) in Brazil. The wind tunnel has a 25 HP/220V electric motor, which drives a 16 rotor-blades that moves the air producing a flow of up to a maximum of 27 m/s in the test-section.

The actual flow velocity in the wind tunnel is measured by a Pitot Tube TPL-06-300 connected

to a pressure transducer model Kimo MP 200. The ambient temperature, relative humidity, barometric pressure is given by a weather station Ecowitt WS 1080CA. Fig.6 illustrates the wind tunnel setup. The wing was mounted on top of a flat surface attached to the end of the wind tunnel test section. The distance of 2.7 c was adjusted to guarantee a uniform flow upstream the model.
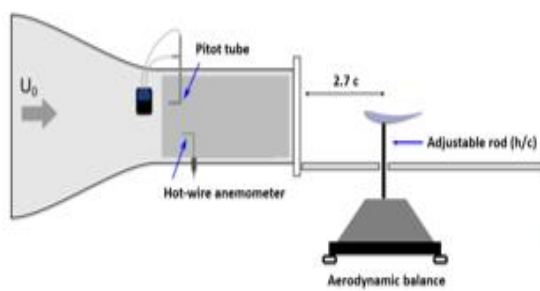
Figure 6. *Wind tunnel setup: (a) schematic assembly; (b) final setup.*

Aerodynamics Force Measurements

The aerodynamic balance used in the experiment was an external balance developed to measure three aerodynamic components: normal force (lift), axial force (drag) and lateral force, in addition to measuring the fundamental momentum of flight: roll, pitch and yaw. It can be seen in Fig. 7 details of this assembly, where the wing is attached to the rod and on the flange connected to the main sting from the aerodynamic balance.

All aerodynamics force readings were software processed and automatically gathered at an acquisition rate of 0.2 s. For each test-run, 300 data samples were collected, and 3 repetitions were performed for each measurement point, according to the test-matrix described in sequence.

Figure 7. *Aerodynamic balance setup.*

Test Matrix

The essays of this work were divided in two tests to better organize the objectives and the results of the work. In both tests the wing was positioned at 2.7 c mm from the wind tunnel exit, as depicted in Fig.6, and the flow speed (22 m/s) was kept constant during both tests. The Reynolds number based on the wing's chord is of order 2.6×10^5.

Test 1: Variation of Height (H/C) and Angle of Attack (α) - Without Endplates

This test was designed to assess not only the relationship between height above the ground and the angle of attack of the airfoil but also to examine two specific heights: 300 mm (h/c = 1.5789) and 38 mm (h/c = 0.2). For each of these heights, five characteristic angles of attack (0°, 4°, 8°, 12°, and 14°) were evaluated to understand aspects such as the maximum C_L/C_D ratio and stall angle. The test aimed to investigate these factors comprehensively.

Test 2: Variation of Height (H/C) and Presence of Endplates - With Fixed A

The goal was to verify and assess data from [1]. This was done using the E423 wing design set with a fixed angle of attack (α = 8°). This angle was chosen because it was reasonably below the aerodynamic stall condition and due to clearance limitations between the wing and the ground.

The experiment involved testing various heights from the floor at the following values:

h_1 = 38 mm (h/c = 0.2); h_2 = 56 mm (h/c = 0.2947); h_3 = 75 mm (h/c = 0.3947); h_4 = 94 mm (h/c = 0.4947); h_5 = 113 mm (h/c = 0.5947); h_6 = 135 mm (h/c = 0.7105); h_7 = 154 mm (h/c = 0.8105); h_8 = 171 mm (h/c = 0.9); and h_9 = 190 mm (h/c = 1.0). Additionally, for each height, the test was conducted both with and without endplates. The objective of this experiment was to quantitatively analyze the interplay between ground effects and the presence or absence of endplates on the wing, with a specific focus on lift and drag.

Measuring Instruments and Accuracy

Accurate measuring instruments play a crucial role in achieving precise results. All the equipment were calibrated and verified before the tests. For measuring the free stream velocity, the error associated is of order 1.4% with a resolution of 0.1 m/s. The aerodynamics forces were obtained with an average error of order 1.5% for lift and 5.6 % for drag. As an application work, like previous investigations [2-5], this study does not delve into extensive details about the measurement techniques.

RESULTS AND DISCUSSION

After processing the data collected through experimental testing, measurements of lift and drag

at various angle of attack (α) and height or ground clearance (h/c) were obtained. These results are illustrated for each test-run, as previously discussed. As is customary in experimental research, potential sources of error were carefully considered. For a more comprehensive and enhanced understanding of the procedure used during the experiment, this section has been subdivided into the following topics: data for test-run 1 showing the variation of height and angle of attack and data for test-run 2 indicating the variation of height with the effect of endplates at a fixed α.

Test-Run 1: Variation of Height (H/C) and Angle of Attack (α)

As test 1 consists of an evaluation of down force (negative lift) and drag as a function of the angle of attack with and without the wing being subjected to ground effect, the results were computed. Remembering that for all tests, Re is within the order of magnitude reported as a low Reynolds number [14] of order $\sim 10^5$. Tables 1 and 2 summarize the results obtained for the height h/c = 1.5789 and h/c = 0.2 respectively, showing some aspects such as the pure average of the lift and drag force, their respective coefficients, and the standard deviation (σ) for the measurements, as a function of the attack angles.

Table 1. *Lift and Drag results for test 1 at h/c = 1.5789.*

α	L (N)	C_L	$\sigma(L)$	D (N)	CD	$\sigma(D)$
0°	−3.8132	-0.1398	1.3560	5.0331	0.1570	0.9345
4°	−13.2745	-0.4865	1.3956	3.2465	0.1190	0.7712
8°	−21.7587	-0.7975	1.3543	3.4029	0.1247	0.6932
12°	−23.7345	-0.8699	1.6243	4.5151	0.1655	0.7847
14°	−21.5455	-0.7897	1.3272	6.2737	0.2299	0.7981

Table 2. *Lift and Drag results for test 1 at h/c = 0.2.*

α	L (N)	C_L	$\sigma(L)$	D (N)	CD	$\sigma(D)$
0°	−9.1556	0.5201	1.3621	2.4335	0.1305	0.7116
4°	−10.0990	0.6311	0.9909	2.7344	0.1243	0.4727
8°	−10.3261	0.7119	1.0118	2.2713	0.1616	0.4719
12°	−12.5284	0.8455	1.3392	4.0620	0.2123	0.8573
14°	−23.7479	1.0010	1.2860	0.3983	0.0912	1.7663

The tests were carried out in an averaged atmosphere with humidity of approx. 82%, temperature of 26°C and barometric pressure of 911 kPa. Expected Re variations during the test-campaign was of order of 1%. Graphs of $-C_L \times \alpha$ and $C_D \times \alpha$ were plotted for test 1, shown in Fig.8, respectively. In Fig. 8(a) it is possible to see a good response in the C_L curve against α parameter. This effect is noticeable when analyzing the C_{Lmax}, which points to a $\alpha_{CLmax} \approx 12°$. After this angle, the lift coefficient

begins to drop, referring to the stall effect. Even though the wing is attached to a rod, at this distance from the ground, the data was insensible to ground effects and the $C_L \times \alpha$ has a standard behavior, as expected for a clean wing. Comparing now the data of h/c = 1.5789 and h/c = 0.2, a very noticeable difference was noticed. For the smallest angles of attack, precisely the angles of 0∘ and 4∘, the lift coefficient for the wing underground effect was significantly higher, as expected by the ground

effect theory registered in literature. However, this behavior is not seen for the two subsequent angles (8° and 12°), which had a slightly lower lift coefficient compared to the same angles for $h/c = 1.5789$. A plausible explanation for this effect comes from the proper interaction of the cambered wing with the upcoming flow under

viscous effects very close to the ground affecting the slope of the $C_L \times \alpha$ curve, which seems to be smoother and progressively increased depending on the angle of attack. However, it is seen that the ground effect delays the stall condition and postpone it to a larger angle of attack ($\alpha > 14°$) in this experiment.
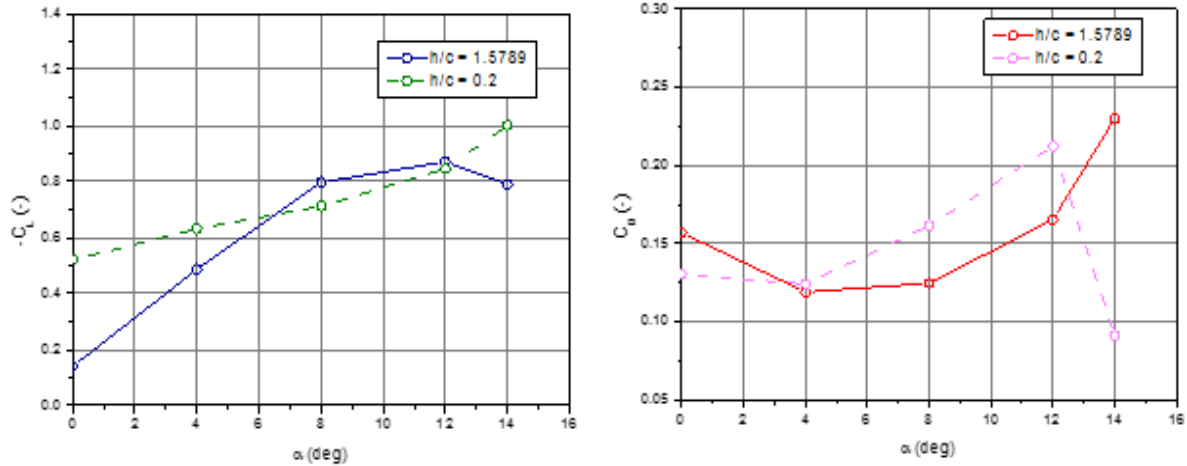
Figure 8. *(a) $-C_L \times \alpha$; (b) $C_D \times \alpha$ for the Test-run 1.*

The drag curve as a function of angle of attack is seen in Fig. 8(b). The data was corrected to consider the drag only for the rod connecting the wing to the aerodynamic balance. However, it must be made clear that as the height increased, more of the rod was subjected to the main flow and some installation or assembly parasitic drag can still be affecting the results.

As for the evolution of the angle of attack and the comparison between the two heights, a similar problem as seen in the downforce ($-C_L \times \alpha$) was encountered. Again, for the first two angles, it is observed that the lower height in relation to the ground causes less drag due to vortex interruptions. However, both angles of 8° and 12° seems to be affected by the flow pattern. Notably, the value of C_D to $\alpha = 14°$ was suddenly reduced. It is important to point out that at this condition, the leading edge of the wing was very close to the ground. Under this flow pattern, it seems that the lift is increased while drag is reduced probably

due to vortex breakdown as registered in [15]. An important point to note is that when analyzing the standard deviation, a considerable increase is observed for the 14° angle, which may suggest either an error in the measurement or an abrupt change in the flow pattern under these conditions, which can be used for a future investigation.

Test-Run 2: Variation of Height (H/C) and Presence of Endplates (With Fixed A)

The main objective of test 2 is to compare the behavior of C_L and C_D as a function of the height (h/c) above the ground, with and without presence of endplates in the wing.

The results tables, with the real distance, dimensionless distance, average of the lift and drag forces for each case, their respective coefficients and standard deviation follow in sequence (tables 3 and 4) with both the presence and absence of endplates.

Table 3. *Lift and Drag results for test 2 at $\alpha = 8°$, without Endplates.*

h	h/c	L (N)	C_L	σ(L)	D (N)	CD	σ(D)
38 mm	0.2000	-19.4234	-0.7119	1.4455	4.4366	0.1626	0.6742
56 mm	0.2947	-24.5941	-0.9014	1.4572	4.5384	0.1663	1.0396
75 mm	0.3947	-26.1836	-0.9596	1.8631	4.4829	0.1643	0.6562
94 mm	0.4947	-25.1920	-0.9233	2.0312	4.4807	0.1642	1.0706
113 mm	0.5947	-23.4653	-0.8600	1.4400	4.4924	0.1646	0.7191
135 mm	0.7105	-23.6827	-0.8680	1.6170	4.6809	0.1716	1.3147
154 mm	0.8105	-23.0031	-0.8431	2.1011	4.5993	0.1686	1.0050
171 mm	0.9000	-22.2641	-0.8160	2.1785	5.0065	0.1835	0.7809
190 mm	1.0000	-22.8151	-0.8362	1.6277	4.9825	0.1826	1.2821

Table 4. *Lift and Drag results for test 2 at α = 8°, with Endplates.*

h	h/c	L (N)	CL	σ(L)	D (N)	CD	σ(D)	Growth in -−CL
38 mm	0.2000	-21.6402	-0.7931	1.5865	4.2935	0.1574	0.6401	11.41%
56 mm	0.2947	-28.2865	-1.0367	2.0017	4.2597	0.1561	0.7978	15.01%
75 mm	0.3947	-28.0974	-1.0298	1.6147	4.3190	0.1583	1.2028	7.31%
94 mm	0.4947	-27.0992	-0.9932	1.7364	4.2566	0.1560	0.8972	7.57%
113 mm	0.5947	-24.7625	-0.9076	2.4956	4.6138	0.1691	1.5483	5.53%
135 mm	0.7105	-25.1690	-0.9225	2.1629	4.6171	0.1692	0.7541	6.28%
154 mm	0.8105	-24.0855	-0.8827	1.9642	4.7714	0.1749	0.8764	4.71%
171 mm	0.9000	-24.3216	-0.8914	1.9541	4.8023	0.1760	1.0175	9.24%
190 mm	1.0000	-23.3480	-0.8557	1.6718	4.8560	0.1780	0.8728	2.34%

Graphs of $-C_L \times h/c$ and $C_D \times h/c$ are plotted in Fig. 9(a)(b) and the wing performance is represented in Fig. 10 as $|C_L/C_D| \times h/c$. The evolution of C_L in relation to the height of the wing had a good correspondence with the trend shown by [1]: for height very close to the ground (in the case of $h/c = 0.2$), the C_L is quite low for both conditions evaluated; then it grows a lot, reaching a peak around $h/c = 0.3 - 0.4$ and slowly decays as the values of h/c increase. Based on the ground effect theory being developed so far, the closer to the ground, the higher the C_L, and this is confirmed by bringing the airfoil closer to the ground up to $h/c \approx 0.3$. However, regions extremely close to the ground tend to greatly reduce the C_L since the down force would be limited by viscous effects [15]; being, therefore, the same reasons and consequences enumerated in test 1 (for the distance of $h/c = 0.2$) that the C_L is reduced. In addition, the presence of the endplate tends to increase the C_L and to reduce the C_D. This causes the downforce peak with endplates to be at a lower h/c than without endplates.
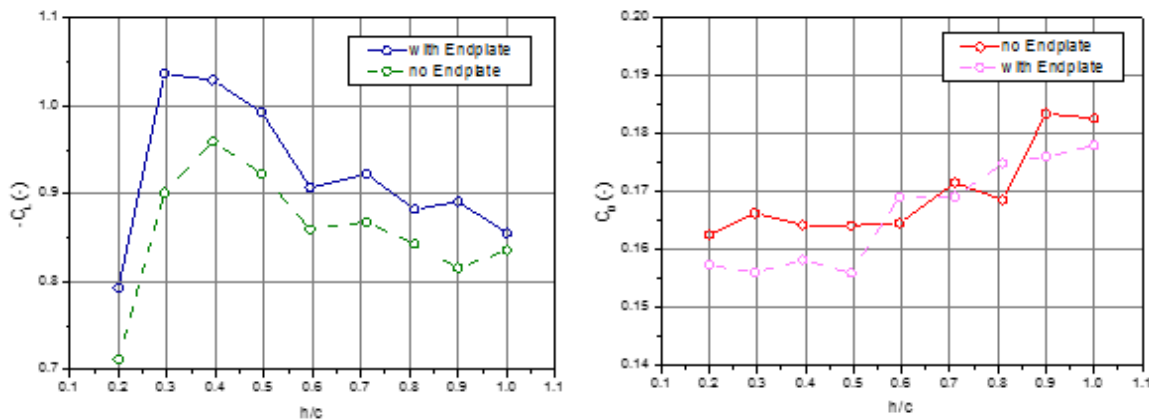
Figure 9. *(a) $- C_L \times h/c$; (b) $C_D \times h/c$ for the Test-run 2 at fixed α = 8°.*

It is possible to see that while in [1] experiment peaks C_L at $h/c \approx 0, 15$; in this experiment such a peak varies about $h/c \approx 0.3$. The reason for this comes from the nature of the E423: a very cambered airfoil, with the chord line passing through it, consequently increasing the absolute value of the height (h/c) as it is measured up to half of its maximum thickness, which is in one of the vertically rearmost parts of the airfoil: at 31% from the chord.

By observing the impact of the presence of endplates, it is possible to note an optimization in the value of C_L. It is evident that there is a consistent increase in this value, as clearly depicted in the graph -$C_L \times h/c$. An endplate has the potential to diminish the induced drag produced by vortices at the wingtip since it aligns with the longitudinal axis of the mean flow, effectively controlling the flow. Consequently, due to the inherent relationship between C_L (lift coefficient) and C_{Di} (induced drag coefficient), the presence of endplates leads to an increase in C_L.

The impact of the presence of endplates is also noticeable in Fig.9(b). A lower C_D can be seen in general for the use of endplates in relation to the wing without them. Theoretically, due to the physical presence of the endplates without any aerodynamic function, the drag should be greater in this case due to the increase in parasitic drag. But precisely because the endplates reduce wingtip vortices [16], the C_{Di} seems to be smaller. However, this trend is more evident at heights (h/c) less than 0.6. A future more detailed investigation is also necessary to completely investigate the effect of the presence of endplates at lower h/c. The optimized relationship between

the downforce and the drag $|C_L/C_D|$ as a function of height (h/c) in relation to the ground is presented in Fig. 10. The trend of the graph is very similar to that of Fig. 9, showing that, for a racing car, increasing the C_L is generally more important than reducing C_D. So much so that there is a big difference, both for the wing without endplates, and for the same one with

endplates, from the $|C_L/C_D|$ from one height to another; referring that the most recommended height from the ground for the E423, subject to a flow velocity of 22 m/s and an angle of attack of 8° is h ≈ 56 mm for the airfoil with endplates and h ≈ 75 mm for it without this accessory. This also proved that the addition of endplates is indispensable for any of the conditions evaluated.
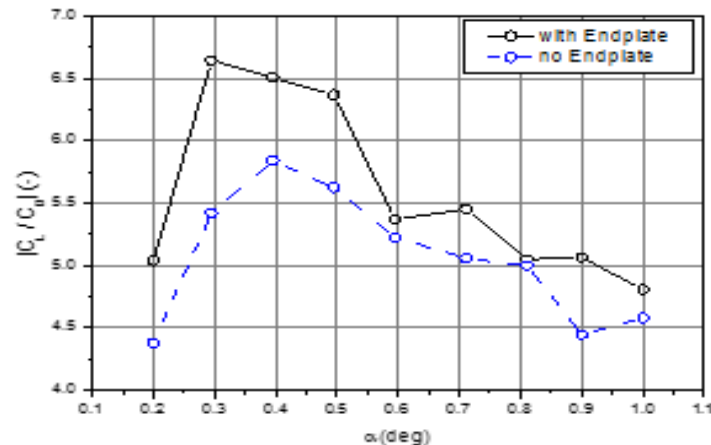
Figure 10. *$|C_L/C_D| \times h/c$ for the Test-run 2 at fixed $\alpha = 8°$.*

CONCLUSION

Many race cars use front wings, typically mounted as close as h/c of 0.1 − 0.3 [1]. A low-aspect ratio wing using an E423 airfoil was studied experimentally using a wind tunnel setup which allowed to vary the ground proximity (h/c). The wing was tested at two different h/c to verify the influence of the ground effect in the $C_L \times \alpha$ and $C_D \times \alpha$ curves. In this situation, C_L had its variation as a function of typical α for an airfoil in an ordinary situation for h/c = 1.5789. However, a different behavior was observed for h/c = 0.2, with a peak of C_L at 14°. Later, as for test 2, the C_L results were consistent with the theory: for small distances (h/c = 0.2), the viscous effects were too predominant to produce enough downforce; however, such effects end up with height increasing a little more, having a peak downforce of $|C_{Lmax}| = 1.0367$) for the wing with endplates and $|C_{Lmax}| = 0.9596$) for it without endplates. As for the drag, the behavior was not so entirely consistent, in general probably due to parasitic drag interfering with the results; but interesting observations can be made that there is a reduction on drag from h/c = 0.2 up to h/c = 0.5, while at the same time lift is augmented, thus improving the aerodynamic efficiency.

A future work should evaluate the variation of the Reynolds number under the same conditions of this work, since the limitation of the speed and dimensions of the wind tunnel caused the Reynolds number to be an order of magnitude

lower than usual for this category of car's wings; causing problems of viscous origin at high angles of attack for test 1. Future development of this research will delve into the following aspects:

- Test with higher AR wings with E423 airfoil.
- Effect of angle of attack when the wing is below h/c = 0.2.
- Detailed flow visualization on the pressure side of the wing to characterize the flow field pattern.
- Investigate the effect of endplate 'shape on the flow pattern and aerodynamic forces at very low h/c values.

REFERENCES

[1] Katz, J. (2006). Aerodynamics of race cars. Annu. Rev. Fluid Mech., 38, 27-63.

[2] Zerihan, J., & Zhang, X. (2000). Aerodynamics of a single element wing in ground effect. Journal of aircraft, 37(6), 1058-1064.

[3] Zhang, X., Toet, W., & Zerihan, J. (2006). Ground effect aerodynamics of race cars. Applied Mechanics Reviews, American Society of Mechanical Engineers, v. 59, p. 32–49.

[4] Hussain, I. Y., & Abood, M. S. (2016). Experimental study of CLARK-Y smoothed inverted wing with ground effect. International Journal of Computer Applications, 147(1), 45-54.

[5] Lu, A., Tremblay-Dionne, V., & Lee, T. (2019). Experimental study of aerodynamics and wingtip vortex of a rectangular wing in flat ground effect. Journal of Fluids Engineering, 141(11), 111108.

[6] Mehraban, A. A., & Djavareshkian, M. H. (2021). Experimental investigation of ground effects on aerodynamics of sinusoidal leading-edge wings. Proceedings of the Institution of Mechanical Engineers, Part C: Journal of Mechanical Engineering Science, 235(19), 3988-4001.

[7] Corfield, E., Hodgson, G., & Garmory, A. (2018). A computational and experimental investigation into the effects of debris on an inverted double wing in ground effect (No. 2018-01-0726). SAE Technical Paper.

[8] Win, S. Y., & Thianwiboon, M. (2021). Parametric optimization of NACA 4412 airfoil in ground effect using full factorial design of experiment. Engineering Journal, 25(12), 9-19. Win, S. Y., & Thianwiboon, M. (2021). Parametric optimization of NACA 4412 airfoil in ground effect using full factorial design of experiment. Engineering Journal, 25(12), 9-19.

[9] Abdizadeh, G. R., Farokhinejad, M., & Ghasemloo, S. (2022). Numerical investigation on the aerodynamic efficiency of bio-inspired corrugated and cambered airfoils in ground effect. Scientific Reports, 12(1), 19117.

[10] Lee, T., & Lin, G. (2022). Review of experimental investigations of wings in ground effect at low Reynolds numbers. Frontiers in Aerospace Engineering, 1, 975158.

[11] Incropera, F. P., DeWitt, D. P., Bergman, T. L., & Lavine, A. S. (1996). Fundamentals of heat and mass transfer (Vol. 6, p. 116). New York: Wiley.

[12] ALLEN, K. R. Wing in ground effect vehicle with endplates. Spruson Ferguson, Level 35 St Martins Tower 31 Market Street, Sydney, NSW, p. 1–59, 2001.

[13] Barlow, J. B., Rae, W. H., & Pope, A. (1999). Low-speed wind tunnel testing. John wiley & sons.

[14] WINSLOW J.; OTSUKA, H. G. B. C. I. Basic understanding of airfoil characteristics at low Reynolds numbers. Journal of Aircraft, Reston (Virginia), v. 55, p. 1–12, 2017.

[15] McBeath, S. (2017). Competition Car Aerodynamics 3rd Edition. Veloce Publishing Ltd.

[16] TOET W.; ZERIHAN, J. Z. X. Ground effect aerodynamics of race cars. Applied Mechanics Reviews, American Society of Mechanical Engineers, v. 59, p. 32–49, 2006.